research articles Journal of proteome research

Human Serum Metabonomic Analysis Reveals Progression Axes for Glucose Intolerance and Insulin Resistance Statuses

Xiuying Zhang,[†] Yulan Wang,[‡] Fuhua Hao,[‡] Xianghai Zhou,[†] Xueyao Han,[†] Huiru Tang,*[,‡] and Linong Ji*[,†]

Department of Endocrinology and Metabolism, Peking University People's Hospital, Peking University Diabetes Centre, Beijing, China 100044, and State Key Laboratory of Magnetic Resonance and Atomic and Molecular Physics, Wuhan Centre for Magnetic Resonance, Wuhan Institute of Physics and Mathematics, The Chinese Academy of Sciences, Wuhan, China 430071

Received June 15, 2009

Understanding the metabolic basis of glucose intolerances and insulin resistance is essential to facilitate early diagnosis, satisfactory therapies and personalized treatments of type 2 diabetes (T2DM). Here, we analyzed the serum metabolic variations from 231 human participants with normal glucose tolerance (NGT, $n = 80$, M/F = 34/46, mean age 53 ± 10 years), impaired glucose regulation (IGR, $n = 77$, M/F = 33/44, mean age 51 ± 10 years) and T2DM ($n = 74$, M/F = 32/42, mean age 51 ± 9 years) to establish the relationship between the serum metabolite compositions and the development of diabetes. By using the proton nuclear magnetic resonance spectroscopy in conjunction with the multivariate data analysis, we found that the development of both glucose intolerances and insulin resistances are closely correlated with the progressive changes of human serum metabonome. Compared with NGT subjects, the IGR and T2DM participants showed clear dysfunctions of choline metabolism, glucose metabolism, lipid and amino acid metabolisms, and disruptions of TCA cycle. The insulin resistance statuses were closely associated with the serum metabonomic changes in terms of glucose, fatty acid and protein/amino acid metabolisms. We also found greater metabonomic heterogeneity among the populations with T2DM and high insulin resistance status. These findings provide useful information to bridge the gaps in our understandings to the metabolic alterations associated with the progression of glucose intolerances and insulin resistance status.

Keywords: glucose intolerance • insulin resistance • metabonomics • NMR • gut microbiota

Introduction

Type 2 diabetes mellitus (T2DM) is a complex polygenic metabolism disorder due to insulin resistance and has become one of the fastest growing public health problems in both developed and developing countries. The World Health Organization estimated that the number of adults with diabetes will be more than doubled from 135 million in 1995 to about 330 million by the year 2025.[1] Population-based studies have shown that the impaired glucose regulation (IGR) is even more prevalent than type 2 diabetes[2] and imposes a great risk in the development of not only T2DM, but also vascular complications.[3] Therefore, the investigation of the molecular alterations related to IGR and the dynamic development processes of glucose intolerance in the systems level is fundamentally important for understanding the mechanisms responsible for the development of T2DM, and subsequent complications and effective treatments.

Recent advances in genomics, transcriptomics, proteomics and metabonomics technologies have offered great opportunities for a more comprehensive understanding of pathophysiology and etiology of complex diseases such as diabetes and obesity.[4] Some human genetic variants associated with increased risk of T2DM have already been discovered using genome-wide association strategy.[5,6] However, the genomic studies alone may not be sufficient for understanding the development of T2DM since the dynamic environmental factors also play important roles in the pathogenesis of diabetes.[7,8] This is clearly indicated in some recent reports that multiple genetic markers fail to provide more power in predicting diabetes than the traditional predictors.[9] Furthermore, although common variants in the fat mass- and obesity-associated (FTO) gene were significantly associated with obesity in European populations, such association was not present for the obesity or T2DM in the Han Chinese population indicating the importance of gene−environment interactions in the development of T2DM.[10]

* To whom correspondence should be addressed. Huiru Tang: State Key Laboratory of Magnetic Resonance and Atomic and Molecular Physics, Wuhan Centre for Magnetic Resonance, Wuhan Institute of Physics and Mathematics, The Chinese Academy of Sciences, Wuhan 430071, PR China. Tel, +86-(0)27-87198430; fax, +86-(0)27-87199291; e-mail, huiru.tang@wipm.ac.cn. Linong Ji: Department of Endocrinology and Metabolism, Peking University People's Hospital, Peking University Diabetes Centre, N0.11, Xi Zhi Men Nan Da Jie, Xicheng District, Beijing 100044, PR. China. Tel, +86-(0)10-88325578; fax, +86-(0)10-88325578; e-mail, E-mail: jiln@bjmu.edu.cn.

[†] Peking University Diabetes Centre.

[‡] Wuhan Institute of Physics and Mathematics.

10.1021/pr900524z CCC: $40.75

Published on Web 08/22/2009

This also suggests that the development of glucose intolerance and diabetes is probably dependent on some environmental factors and is thus population-dependent.

Metabonomics studies on different populations ought to be crucial since metabonomics can provide holistic metabolism (metabonome) information for the pathogenesis[11] resulting from both genetic and environmental factors.[12] Metabonomics approaches combine the metabolic profiles of biofluids obtained from nuclear magnetic resonance (NMR) spectroscopy and/or mass spectrometry (MS) with multivariate data analysis techniques. In fact, metabonomics has already been widely applied to understand the molecular aspects of stresses,[13] carcinogenesis,[14] drug toxicology[15] and environmental sciences.[16] Potential biomarkers have been explored and identified for a number of diseases, such as hepatocellular carcinomas[17] and brain cancers,[18] cardiovascular diseases[19] and parasitic diseases.[20−22]

A number of investigations have been reported to understand the diabetes related metabolic alterations. In the early 1980s, NMR spectroscopic analysis of plasma and urine demonstrated the usefulness of metabolic profiling in these aspects by revealing the altered blood glucose metabolism and ketogenesis in diabetes patients.[23] More recently, metabolism alterations in fatty acids, organic acids and phospholipids were found to be responsive to diabetes and drug interventions.[24−26] Metabonomic investigations further showed associations between the alterations in gut microflora and fatty liver[27] probably through altered gut microbiota modulations on host metabolisms.[28,29] Furthermore, metabonomic studies revealed many changes of human plasma metabonome associated with diabetic kidney diseases, insulin resistance and glucose challenge induced metabolic responses from prediabetes.[30,31] However, these works were either aimed at developing methods for diabetes diangosis or based on limited cases without careful exclusion of relevant conditions. Similar studies focused on the Han Chinese populations remain to be carried out, especially with the new findings on the population dependence of T2DM.[10] Comprehensive understanding of the metabolic characteristics associated with different glucose tolerance and insulin resistance statuses also remains to be achieved.

In this report, we analyzed the serum metabonomic characteristics of the age- and sex-matched Han Chinese population with normal glucose tolerance (NGT), IGR and T2DM using the metabonomics approach based on the combination of NMR spectroscopy and multivariate data analysis. The aims of this study are to explore the relationships between the serum metabonome and the glucose intolerance and insulin resistance statuses with a view to provide more insights into metabolic progression associated with the development of glucose intolerance and insulin resistance in a Han Chinese population.

Experimental Methods

Study Subjects and Sample Collection. The study subjects were recruited in Beijing as part of a project entitled "The nationwide survey of the prevalence of type 2 diabetes and metabolic syndrome" project. All participants were adults of Han ethnic residents in Beijing region without hypertension, renal or liver dysfunction. The study protocol was in accordance with the Helsinki declaration and approved by the ethics committee of Peking University with written informed consent from all participants. To focus on the objectives of this study and exclude the effects of age, gender, and obesity, a total of 231 age-, gender-, and body mass index (BMI)-matched participants were selected and divided into three groups according to WHO criteria of diagnosis of diabetes.[32] These groups are participants with NGT ($n = 80$, M/F = 34/46, mean age 53 ± 10 years), IGR, including subjects with impaired fasting glucose and/or impaired glucose tolerance ($n = 77$, M/F = 33/44, mean age 51 ± 10 years), and T2DM ($n = 74$, M/F = 32/42, mean age 51 ± 9 years). Among the T2DM group, 48 patients were newly diagnosed thus without any treatments; another 26 patients were only treated with short-acting oral hypoglycemic drugs (in the form of monotherapy) about 10−14 h prior to sampling; these drugs include metformin hydrochloride, acarbose, glipizide or repaglinide (with inefficient glycemic control). For NGT and IRG groups, no lifestyle or drug interventions were introduced prior to taking the blood samples.

Venous blood samples were taken from individuals after overnight fasting for at least 10 h and the serum samples were obtained in the normal manner. Aliquots of serum samples were snap frozen in liquid nitrogen, and stored at −80 °C until NMR analysis was performed. Oral glucose tolerance test (OGTT) was performed for each participant by measuring plasma glucose levels at 0 and 2 h after oral ingestion of 75 g of glucose.

Clinical Chemistry Measurements. Serum total cholesterol (CH), low-density lipoprotein cholesterol (LDL-C), high-density lipoproteins cholesterol (HDL-C) and triglycerides (TG) were measured using an automatic biochemical analyzer (Olympus AU640). The level of fasting insulin (FINS) was determined using the ADVIA Centaur immunoassay system (Fernwald, Germany) according to the manufacturer's instruction. The insulin resistance index (IR) was calculated from the fasting plasma glucose (FPG, mmol/L) and insulin values (FINS, μU/mL) as HOMA-IR = FPG*FINS/22.5.[33]

NMR Spectroscopic Analysis. For NMR analysis, 400 μL of serum samples was mixed with 200 μL of 0.9% NaCl (w/v) solution containing 50% D_2O (as a field lock) followed with 10 min centrifugation at 10 000 rpm with a benchtop centrifuge. A total of 550 μL of the supernatant of each sample was then transferred into a 5 mm high quality NMR tube individually. All NMR spectra were recorded at 298 K on a Bruker AVIII 600 spectrometer (Bruker Biospin, Germany) equipped with a cryogenic probe operating at 600.13 MHz for ^{1}H and 150.91 MHz for ^{13}C, respectively.

For each sample, two spectra were recorded including a standard one-dimensional spectrum and a spin−spin relaxation (T_2) edited spectrum using NOESYPR1D pulse sequence (RD-90-t_1-90-t_m-90-acqusition) and Carr−Purcell−Meiboom−Gill[34] (CPMG, RD-90°-(τ-180°-τ)$_n$-acquisition) sequence, respectively. In both experiments, the 90° pulse length was set to about 10 μs; a total of 32 FIDs (free induction decay) were collected into 32k data points with a spectral width of 20 ppm and the recycle delay (RD) of 2 s. Water signal was saturated with a weak irradiation during the recycle delay and mixing time (t_m) of 100 ms; t_1 was set to 3 μs. In the CPMG experiments, the τ value was 350 μs and the relaxation delay ($2n\tau$) was 35 ms. With these parameters, the lipid signals were attenuated only to assist observation of small metabolites and were still included in multivariate data analysis (see Figure 1). Assuming small intergroup variations for the T_2 values of the lipid species, little effects on the data analysis results of these biochemical species are expected for such CPMG parameters.

For spectral assignment purposes, two-dimensional NMR (2D NMR) spectra were recorded for selected samples including ^{1}H−^{1}H correlation spectroscopy (COSY), total correlation spec-

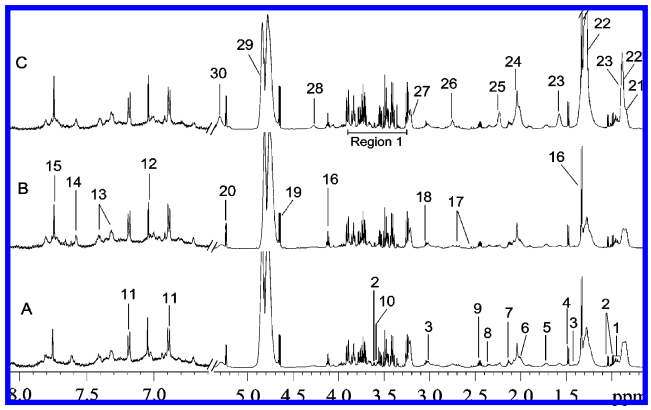

Figure 1. 600 MHz CPMG ^{1}H NMR spectra of human serum samples with (A) normal glucose tolerance, (B) impaired glucose regulation and (C) type2 diabetes (the region at δ6.5−8.0 was expanded for 32 times). The area labeled "region 1" in spectra C contains signals from glucose, lipid and amino acids. Keys: 1, leucine/isolucine (Leu/Ile); 2, valine (Val); 3, lysine (Lys); 4, alanine (Ala); 5, arginine (Arg), leucine, lysine; 6, proline (Pro); 7, methionine (Met); 8, glutamate (Glu); 9, glutamine (Gln); 10, threonine (Thr); 11, tyrosine (Tyr); 12, methylhistidine; 13, phenylalanine (Phe); 14, 3-methylhistidine; 15, histidine (His); 16, lactate; 17, citrate; 18, creatinine; 19, β-glucose (Glc); 20, α-glucose; 21, HDL; 22, LDL; 23, VLDL; 24, Glycoprotein; 25, lipid; 26, lipid; 27, choline; 28, glyceryl of lipid; 29, water; 30, unsaturated lipid.

troscopy (TOCSY) and J-resolved NMR spectra. ^{1}H−^{1}H COSY 2D NMR spectra were recorded with the gradient selected pulse sequence, while ^{1}H−^{1}H TOCSY 2D NMR spectra were acquired with MLEV17 as the spin-lock scheme and mixing time of 80 ms. In both cases, 128 increments were acquired and each increment was featured with 2048 data points and the spectral width of 10.5 ppm in both dimensions. The data were zero-filled into 2048 data points for both dimensions prior to Fourier Transformation (FT). The J-resolved spectra were recorded with 50 increments and each increment was defined with 4096 data points and spectral-width of 10.5 ppm.

Spectral Processing and Analysis. The FIDs for one-dimensional data were zero-filled to 128k and multiplied by an exponential function with the line-broadening factor of 0.5 Hz prior to FT. The NMR spectra were then corrected for phase and baseline distortions using Topspin (Version 2.0, Bruker Biospin) and referenced to the doublet of α-glucose (δ5.23). The region δ0.5−9.5 was divided into 2833 integral segments with the width of 0.003 ppm (1.8 Hz) using AMIX software package (V3.8.3, Bruker Biospin, Germany). The regions at δ4.09−4.21, δ4.32−5.17, and δ5.50−6.50 were discarded to eliminate the effects of imperfect water saturation and the urea signals. The spectral data were then normalized to a constant sum for each spectrum.

Multivariate data analysis was performed with the software SIMICA-P+ (v11.0, Umetric, Umea, Sweden). Principal component analysis (PCA), partial least-squares-discriminant analysis (PLS-DA) and the orthogonal projection to latent structure with discriminant analysis (OPLS-DA)[35] were employed sequentially to find outliers and to extract the statistically significant metabolite changes related to this study. OPLS-DA models were calculated with unit variance scaling (UV) and the results were visualized in the forms of scores plots to show the group clusters and loadings plots to show variables (NMR signals) contributing to clustering; the loadings obtained were back-transformed before generating the coefficient-coded loadings plots,[36] where variables were color-coded with the absolute values of the Pearson correlation coefficients (r), using a Matlab script (V7.0, The Math-works, MA) downloaded (http://www.mathworks.com/) and modified in-house by Dr Zhu Hang. A 7-fold cross-validation was applied to all PLS and OPLS models and the reliabilities of models were further rigorously validated by permutation tests[37] with a permutation number of 200. Since OPLS-DA results obtained from the NOESYPR1D NMR spectra are similar to those from CPMG NMR spectra, only the detailed analysis for the CPMG spectra will be discussed in the Results and Discussion.

Table 1. The Clinical Data for Normal Glucose Tolerance (NGT), Impaired Glucose Regulation (IGR), and Type 2 Diabetes (T2DM) Groups

clinical indicator	NGT (N = 80)	IGR (N = 77)	T2DM (N = 74)
Sex (M/F)	34/46	33/44	32/42
Age (year)	51 ± 9[a]	51 ± 10	53 ± 10
BMI (kg/m^2)	25.1 ± 2.3	25.9 ± 2.7	25.9 ± 3.0
SBP (mmHg)	127 ± 14	129 ± 15	130 ± 15
DBP (mmHg)	77 ± 8	79 ± 8	78 ± 8
FPG (mmol/L)	5.44 ± 0.39	5.96 ± 0.53	9.20 ± 2.93[c,d]
2hPG (mmol/L)	5.54 ± 1.23	8.27 ± 1.33[b]	17.2 ± 6.9 [c,d]
CH (mmol/L)	4.57 ± 0.78	4.85 ± 0.97	4.74 ± 1.11
TG (mmol/L)	1.28 ± 0.61	1.45 ± 0.75	1.86 ± 1.18[c,d]
HDL-C (mmol/L)	1.27 ± 0.25	1.26 ± 0.28	1.14 ± 0.28 [c,d]
LDL-C (mmol/L)	2.45 ± 0.66	2.77 ± 0.72[b]	2.70 ± 0.87[c]
FINS (MIU/L)	6.59 ± 3.15	8.83 ± 5.0[b]	8.14 ± 4.26[c]
IR	1.61 ± 0.82	2.36 ± 1.43[b]	3.10 ± 1.55[c,d]

[a] Means ± SD. [b] $P < 0.05$ for IGR vs NGT. [c] $P < 0.05$ for T2DM vs NGT. [d] $P < 0.05$ for T2DM vs IGR.

Results

Clinical Chemistry. The clinical chemistry data (Table 1) showed that FPG, plasma glucose 2 h after oral glucose challenge (2hPG), TG, LDL-C, FINS and IR values are all significantly higher in T2DM patients than in the NGT group ($p < 0.05$), whereas HDL-C level is lower in T2DM patients than in NGT and IGR groups. LDL-C, 2hPG, FINS and IR values for the IGR participants are also higher than those for NGT group.

^{1}H NMR Spectroscopy of Serum Samples. Figure 1 shows three typical ^{1}H CPMG NMR spectra for human sera from individuals with NGT (Figure 1A), IGR (Figure 1B), and T2DM (Figure 1C), respectively. The NMR resonances were assigned according to the literature data[38,39] and further confirmed with 2D NMR results. Similar to the published observations,[39] our cohort samples mainly contained glucose, a range of amino acids, some organic acids, lipids, choline and creatinine. Clear differences in triglyceride levels (peak 28) can be observed between the T2DM and NGT groups. However, in order to recover the characteristics of metabolic patterns of participants with T2DM and IGR, multivariate data analysis of NMR spectra was subsequently performed.

Multivariate Data Analysis of NMR Data. To determine whether the short-acting hypoglycemic drug treatments had any lasting impacts on the serum metabolic profiles, PCA and OPLS-DA were performed for the NMR data obtained from two T2DM subgroups including the newly diagnosed or untreated (n = 48) and T2DM patients subjected to treatment with short-acting oral hypoglycemic agents (n = 26). The PCA and OPLS-DA scores plots (Supplementary Figure S1A and S1B) showed no significant differences between the serum metabonome of these two subgroups. This is also consistent with the findings

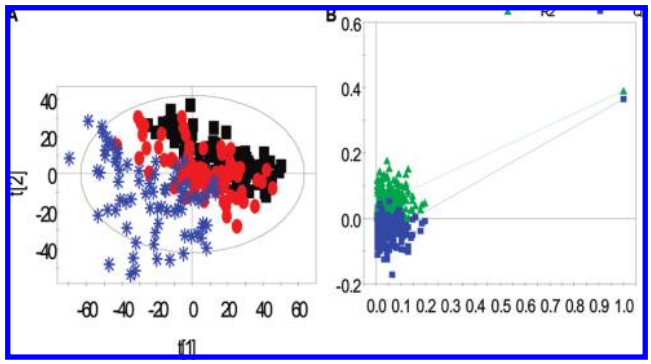

Figure 2. (A) PLS-DA scores plot ($R^2 = 0.52$, $Q^2 = 0.33$) for normal glucose tolerance (NGT, $n = 80$, black squares), impaired glucose regulation (IGR, $n = 77$, red dots), and type 2 diabetes (T2DM, $n = 74$, blue stars). (B) Permutation test plot for the PLS-DA model (number of permutations, 200; intercepts: $R^2 = 0.0, 0.03$; $Q^2 = 0.0, -0.06$).

from the fasting blood glucose data which showed no significant differences for these two subgroups (9.88 ± 3.09 vs 8.83 ± 2.80 mmol/L, $P > 0.05$). This is probably due to the short-acting nature of these drugs with respect to the time scale of long fasting. Therefore, in the subsequent comparative metabonomic analysis, these two subgroups were treated together as a single group (T2DM group).

PLS-DA was conducted for all three groups, namely, NGT, IGR and T2DM, using NMR data as **X**-matrix and the class information as the **Y**-matrix with two PLS components calculated (R^2X, 0.52; Q^2Y, 0.33). The scores plot (Figure 2A) clearly showed an axis of glucose intolerance progression from NGT to IGR and further to T2DM groups. The result of permutation test indicated that this PLS-DA model was reliable in explaining and predicting the variations in **X** and **Y** matrix (Figure 2B, intercepts: $R^2 = 0.0, 0.03$; $Q^2 = 0.0, -0.06$).

To further identify the significant serum metabonomic differences between three different groups representing different glucose tolerance statuses, pairwise comparative OPLS-DA analyses were conducted with one orthogonal and one predictive component calculated for each of the models. The results are displayed in the forms of scores plots and corresponding loadings plots with color-coded correlation coefficients of metabolites (Figure 3). The observed phase (positive or negative) of the resonance signals represents the relative (increase or decline) changes in the concentration of metabolites. The hot colored metabolites (e.g., red) show more significant contribution than the cold colored (e.g., blue) ones for the intergroup discrimination. In this study, a correlation coefficient of $|r| > 0.23$ was used as the cutoff value for the statistical significance based on the discrimination significance at the level of $p < 0.05$, which was determined according to the discriminating significance of the Pearson's product-moment correlation coefficient.[36] The discriminating metabolites and corresponding coefficients with different glucose tolerance status are summarized in Table 2.

The OPLS-DA scores plot showed clear separation (with R^2X=0.55, $Q^2Y = 0.76$) between the T2DM patients and NGT groups (Figure 3A). The corresponding loadings plot revealed that, compared with NGT group, the T2DM sera contained significantly higher levels of glucose together with lower levels of citrate, lactate and some amino acids including alanine, leucine, isoleucine, valine, methionine, proline, lysine, tyrosine, histine and glutamine. In addition, T2DM group contained lower concentrations of HDL-C and choline than the NGT group (Table 2). Good serum metabonomic differentiation is also evident for the IGR and T2DM groups ($R^2X = 0.54$, $Q^2Y = 0.57$) (Figure 3B). The corresponding coefficient-coded loadings plot indicated that, compared with IGR group, the sera of T2DM group had significantly higher concentration of glucose but lower concentrations of lactate, citrate, HDL-C, choline and some amino acids including alanine, isoleucine, histidine and glutamine. Furthermore, the metabonomic differences between IGR and NGT groups ($R^2X = 0.48$, $Q^2Y = 0.40$) are visible in the OPLS-DA scores plot (Figure 3C). Detailed analysis suggests that, compared with NGT group, the sera of IGR group has relative higher levels of glucose but lower levels of lactate and some amino acids including alanine, histidine and glutamine. However, it is worth noting that the serum metabonomic differences between IGR and NGT groups are much less drastic than those between IGR and T2DM groups. The permutation tests showed that all the above pairwise comparative OPLS-DA models are of good quality and reliability (Supplementary Figure S2A−C). Moreover, the T2DM group showed greater intragroup metabonomic differences than the other two groups.

To find out whether the serum metabonomic features are associated with the IR index throughout these three groups, we calculated an OPLS model (Figure 4) using NMR data as **X**-matrix and IR values as **Y**-matrix with one PLS and one orthogonal component ($R^2X = 0.52$, $Q^2Y = 0.16$). The PLS scores plot of such model (Figure 4A) showed three distinct groupings for participants with low IR (0.40−1.40, black squares), intermediate IR (1.41−2.80, red dots) and high IR values (2.81−7.75, blue triangles), indicating the presence of association between the serum metabonome and the insulin resistance statuses. It is further noted that the high IR group has an obviously greater intragroup variations probably indicating a greater metabonomic heterogeneity than the other two groups. The corresponding coefficient-coded loadings plot (Figure 4B) showed that, with the increase of IR values, the concentrations of glucose and VLDL were increased, whereas the levels for HDL-C, lactate, choline, citrate and several amino acids including alanine, valine, leucine and glutamine were decreased. The permutation test result also indicated that this OPLS model was reliable (Supplementary Figure S3).

Discussion

The above observations indicate that the NMR-based metabonomics approach is feasible to analyze the metabonomic differences between different insulin resistance and glucose intolerance statuses including NGT, IGR and T2DM groups. Such approach is also useful to pin down the important metabolic pathways which may play vital roles in the development of diabetes. Furthermore, this study showed a clear metabonomic trajectory with the increase of the insulin resistance (Figure 4A) and for glucose intolerance from NGT to IGR and further to T2DM (Figure 2), probably indicating the presence of a continuous progressive development axis for the insulin resistance and the glucose intolerance severity. Although this observation coincides, to some extent, with the changes of fasting blood glucose, our results revealed more details in the metabolic complexity of insulin resistance and glucose intolerance statuses than glucose measurement alone, especially when the NGT and IGR groups were concerned. Such progressive development is not surprising since an individual with IGR may take some years to become T2DM depending on the lifestyles and genetic background. These results also

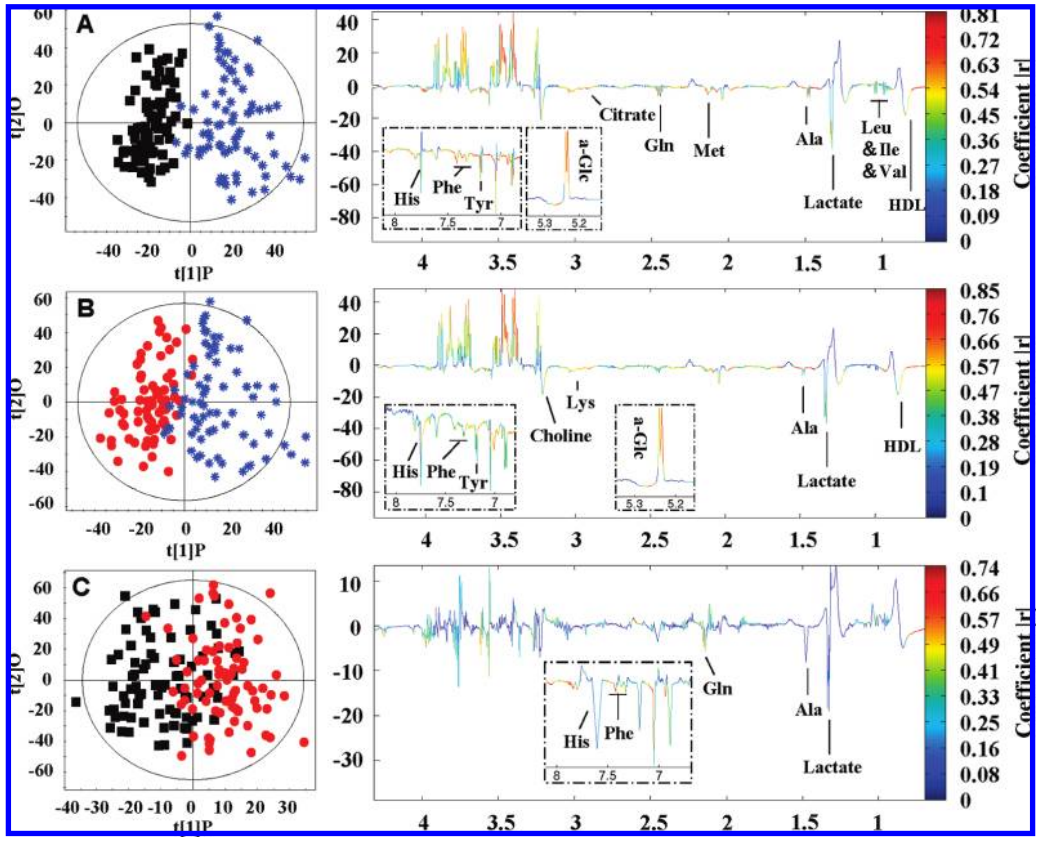

Figure 3. OPLS-DA scores plots and regression coefficient plots for (A) T2DM (blue stars, positive) and NGT groups (black squares, negative), (B) T2DM (blue stars, positive) and IGR groups (red dots, negative), and (C) IGR (red dots, positive) and NGT groups (black squares, negative). $|r|$ represents the scale for the coefficients of the variables contributing to the group classifications.

Table 2. The Significantly Changed Metabolites Related to the Different Glucose Intolerance Status ($|r| > 0.23$, $p < 0.05$)

metabolites	changes in IGR (vs NGT)	changes in T2DM(vs IGR)	changes in T2DM(vs NGT)
HDL		↓	↓
Isoleucine			↓
Leucine			↓
Valine			↓
Alanine	↓	↓	↓
Methionine			↓
Glutamine	↓	↓	↓
Citrate		↓	↓
Lysine		↓	↓
Choline		↓	↓
Lactate	↓	↓	↓
Tyrosine	↓	↓	↓
Phenylalanine	↓	↓	↓
Histidine	↓	↓	↓
Glucose		↑	↑

suggest that the dysfunction of glucose homeostasis is a progressive process accompanied with many metabolic changes and there may not be a clearly defined boundary for glucose intolerances. Furthermore, the progressive changes of serum metabonome are correlated with the insulin resistance suggesting the close association between development of insulin resistance and the serum metabonomic changes in a holistic manner.

The Changes of Glucose Metabolism. In this study, one of the most obvious observations is the marked elevation of blood glucose level together with reduced levels of the citrate and lactate levels in T2DM and IGR groups in comparison with the NGT group; the concentration of citrate was also lower in T2DM patients than in IGR individuals (Figure 3). This suggests the disturbance of glycolysis and TCA cycle in IGR and T2DM groups and the severity of such disturbance increased from IGR to T2DM. Since citrate is one of the most important TCA cycle intermediates, its depletion indicates a reduction of the aerobic glycolysis. Insulin plays a major role in the uptake of glucose into muscle and adipose tissue, and facilitates anaerobic and aerobic glycolysis. Insulin resistance and insufficient insulin secretion often lead to the weakened glycolysis and subsequent elevation of glucose and reduced production of citrate and lactate (Figure 5). Furthermore, insulin resistance leads to reduced rate of muscle glycogen synthesis and, hence, accumulation of glucose in the blood circulation. In the current investigation, we found a direct and positive correlation between the levels of serum glucose and IR index and a negative correlation between the levels of citrate, lactate and IR (Figure 4), supporting the notion that insulin resistance is associated with disturbed metabolism of glucose and TCA cycle.[40] However, the changes of the lactate levels are inconsistent with these previously reported[41] probably for a number of reasons. The medical history of participants enrolled may contribute to such discrepancy; in our investigation, most participants in T2DM groups were diagnosed for the first time and had not been previously treated, whereas other studies did not report the stage of disease development and treatment histories. Different sampling methods in the premeasurement procedures could also contribute to the variations in the levels of lactate. Although our study adopted a similar sampling

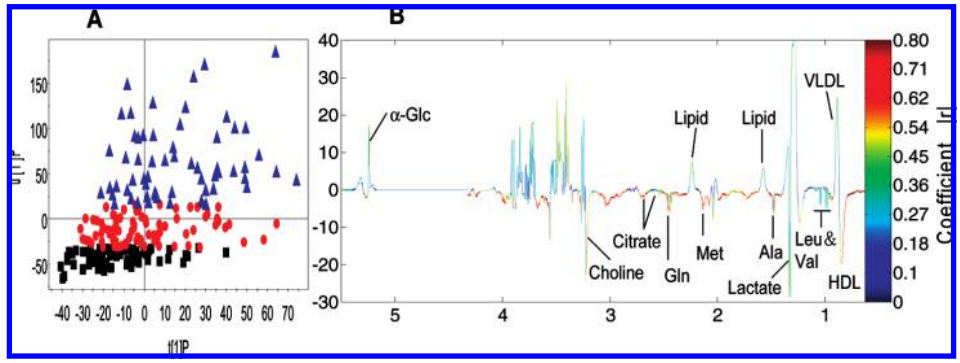

Figure 4. OPLS scores plot (A) and regression coefficient plot (B) for the correlation between NMR data and insulin resistance (IR) index including low IR (black squares), intermediate IR (red dots), and high IR (blue triangles).

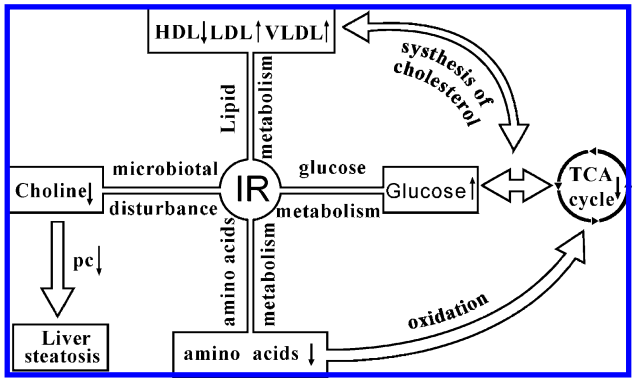

Figure 5. An overview of the metabolic pathway alterations related to the glucose intolerance and insulin resistance statuses.

method for all three groups, further investigation is clearly warranted to confirm the lactate changes.

The Changes of Amino Acids Metabolism. In this study, we have observed a declined level of a range of amino acids in T2DM patients (Table 2) which is consistent with the previously reported results. For example, in a cross-sectional study of the first-degree relatives of T2DM parents,[42] fasting hyperinsulinemia and lower levels of amino acids such as alanine, serine, glutamine and glycine were observed in the plasma of the offspring of diabetic parents. The reduced levels of amino acids observed in T2DM could be explained by altered energy metabolism as well. Since the utilization of carbohydrate is impaired to some extent in IGR and T2DM, the oxidation of amino acids becomes an alternative energy source by entering TCA cycle at different points. In addition, the conversion of amino acids into glucose *via* gluconeogenesis can be enhanced in T2DM patients (Figure 5). The reduced levels of amino acids in T2DM patients are also partially related to the alterations in the rate of protein turnovers, which is confirmative evidence for the reported elevations in protein flux, synthesis and breakdown with the net balance diminished in patients with T2DM.[43]

Insulin has an important regulatory function in the supply of amino acids from muscle protein for gluconeogenesis. In this study, a negative correlation between the levels of amino acids and IR was observed (Figure 4). When the balance between the level of insulin and Glucagon is disturbed, amino acids become one of the most important precursors for gluconeogenesis. Impaired insulin secretion also promotes the direct gluconeogenesis from amino acids and results in the increases in the level of glucose.[44] This may in turn explains the observed decreases in a range of amino acids in the serum of T2DM patients. The findings observed here suggest that the perturbations in amino acids are complex in the progression of diabetes even though the proteolysis, gluconeogenesis and oxidative catabolism are probably the major relevant pathways. Nevertheless, further studies are clearly in demand to elucidate the roles of the amino acid metabolism in both the development and management of diabetes.

The Changes of Lipid Metabolism. Insulin resistance and T2DM are often associated with lipid metabolism disorders such as hypertriglyceridemia, elevation of LDL and alleviation of HDL cholesterol. Our findings are in good agreement with those mentioned above (Figure 4). Such findings are also confirmed by the clinical chemistry data obtained in this study (Table 1). A similar observation was reported[45] that insulin resistance had close association with the concentrations for VLDL, LDL, and HDL cholesterol in T2DM patients. Other studies have also reported the connection between insulin sensitivity and the level of HDL-C in patients with T2DM by increasing hepatic secretion of triglyceride-rich VLDL particles and by impairing the clearance of lipoprotein particles from plasma.[46]

Furthermore, we observed that the decline of serum choline level was associated with T2DM and the increases in the IR values (Figure 4). Since choline is an important precursor of phosphorycholine that is a necessary component for assembly and secretion of VLDL, lack of choline can lead to accumulation of TG in the liver, causing liver steatosis (Figure 5). Coincidently, the prevalence of nonalcoholic fatty liver has found to be associated with T2DM patients[47] and a choline-deficiency diet can cause hepatic steatosis,[48] which is reversible by choline intravenous infusion. A possible microbiota involvement in choline metabolism was proposed[27] with the observation of an increased level of methylamines, a microbiota-mediated choline metabolite, in the urine of high fat diet-induced insulin resistance mice. Therefore, it is possible that alterations of gut microbiotal activities may have important implications in the development of diabetes. It is particularly worth mentioning that greater metabonomic variations are present for the T2DM group than the other two groups and for the high IR group clearly indicating the marked metabonomic heterogeneity in T2DM and high IR groups. The details are in need of further investigation.

Conclusions

Clear metabolic differences are present between different glucose intolerance statuses including NGT, IGR and T2DM and

different insulin resistance statuses. The metabonomic changes are closely associated with the progressive development of insulin resistance status and the glucose intolerance severity. The metabonomic alterations associated with glucose intolerance and insulin resistance status are highlighted by the dysfunction of glucose and lipid metabolism, and oxidative catabolism of amino acids. The alterations of choline metabolism noticed in T2DM patients imply the importance of changes in gut microbiotal activity in diabetic development. The combination of these metabolism alterations and associated biomarkers such as glucose, lipoproteins, citrate and amino acids may collectively hold promise for early prediction and diagnosis for the development of T2DM and insulin resistance. Our study also demonstrates that the NMR-based metabonomics approach is feasible for rapid and high-throughput investigation of other metabolic disorders to provide insight into the metabolic mechanism underlying the disease development and facilitate the efficient delivery of personalized medicine.

Abbreviations: COSY, correlation spectroscopy; CPMG, Carr−Purcell−Meiboom−Gill; FID, free induction decay; FINS, fasting insulin; FPG, fasting plasma glucose; FT, Fourier Transformation; IGR, impaired glucose regulation; IR, insulin resistance index; NGT, normal glucose tolerance; NMR, nuclear magnetic resonance; OGTT, Oral glucose tolerance test; OPLS-DA, orthogonal partial least-squares-discriminant analysis; PCA, principal components analysis; PLS, partial least-squares; TOCSY, total correlation spectroscopy; T2DM, type 2 diabetes.

Acknowledgment. We acknowledge the financial supports from the National Basic Research Program of China (2006CB503900, 2007CB914701), National High Technology Research and Development Program (2006AA-02A409), the National Natural Science Foundation of China (20825520) and the Knowledge Innovation Program of the Chinese Academy of Sciences (KSCX1-YW-02). We thank all the participants for agreeing to join this study and the staff at Peking University Diabetes Centre who aided in this study. We also thank Dr. Hang Zhu, Wuhan Institute of Physics and Mathematics, for modifying the MatLab scripts for color-coding the coefficients.

Supporting Information Available: Scores plot of PCA model resulting from the ^{1}H NMR spectra of T2DM with and without hypoglycemic agents; OPLS-DA scores plot for T2DM with and without treatment; the permutation test plots for the OPLS-DA models for classification of T2DM and NGT groups, T2DM and IGR groups, and IGR and NGT groups; the permutation test plots for the OPLS model for correlation between NMR data and IR values. This material is available free of charge via the Internet at http://pubs.acs.org.

References

(1) International Diabetes Federation. *Diabetes Atlas*, 3rd ed. [Online]; IDF Executive Office: Brussels , 2006. http://www.eatlas.idf.org.
(2) Nathan, D. M.; Davidson, M. B.; DeFronzo, R. A.; Heine, R. J.; Henry, R. R.; Pratley, R.; Zinman, B. Impaired fasting glucose and impaired glucose tolerance: implications for care. *Diabetes Care* **2007**, *30* (3), 753–759.
(3) Santaguida, P. L.; Balion, C.; Hunt, D.; Morrison, K.; Gerstein, H.; Raina, P.; Booker, L.; Yazdi, H. Diagnosis, prognosis, and treatment of impaired glucose tolerance and impaired fasting glucose. *Evid. Rep. Technol. Assess. (Summ.)* **2005**, *128*, 1–11.
(4) Collins, C. D.; Purohit, S.; Podolsky, R. H.; Zhao, H. S.; Schatz, D.; Eckenrode, S. E.; Yang, P.; Hopkins, D.; Muir, A.; Hoffman, M.; McIndoe, R. A.; Rewers, M.; She, J. X. The application of genomic and proteomic technologies in predictive, preventive and personalized medicine. *Vascul. Pharmacol.* **2006**, *45* (5), 258–267.
(5) Scott, L. J.; Mohlke, K. L.; Bonnycastle, L. L.; Willer, C. J.; Li, Y.; Duren, W. L.; Erdos, M. R.; Stringham, H. M.; Chines, P. S.; Jackson, A. U.; Prokunina-Olsson, L.; Ding, C. J.; Swift, A. J.; Narisu, N.; Hu, T.; Pruim, R.; Xiao, R.; Li, X. Y.; Conneely, K. N.; Riebow, N. L.; Sprau, A. G.; Tong, M.; White, P. P.; Hetrick, K. N.; Barnhart, M. W.; Bark, C. W.; Goldstein, J. L.; Watkins, L.; Xiang, F.; Saramies, J.; Buchanan, T. A.; Watanabe, R. M.; Valle, T. T.; Kinnunen, L.; Abecasis, G. R.; Pugh, E. W.; Doheny, K. F.; Bergman, R. N.; Tuomilehto, J.; Collins, F. S.; Boehnke, M. A genome-wide association study of type 2 diabetes in Finns detects multiple susceptibility variants. *Science* **2007**, *316* (5829), 1341–1345.
(6) Sladek, R.; Rocheleau, G.; Rung, J.; Dina, C.; Shen, L.; Serre, D.; Boutin, P.; Vincent, D.; Belisle, A.; Hadjadj, S.; Balkau, B.; Heude, B.; Charpentier, G.; Hudson, T. J.; Montpetit, A.; Pshezhetsky, A. V.; Prentki, M.; Posner, B. I.; Balding, D. J.; Meyre, D.; Polychronakos, C.; Froguel, P. A genome-wide association study identifies novel risk loci for type 2 diabetes. *Nature* **2007**, *445* (7130), 881–885.
(7) Pandey, A.; Mann, M. Proteomics to study genes and genomes. *Nature* **2000**, *405* (6788), 837–846.
(8) Ideker, T.; Thorsson, V.; Ranish, J. A.; Christmas, R.; Buhler, J.; Eng, J. K.; Bumgarner, R.; Goodlett, D. R.; Aebersold, R.; Hood, L. Integrated genomic and proteomic analyses of a systematically perturbed metabolic network. *Science* **2001**, *292* (5518), 929–934.
(9) Meigs, J. B.; Shrader, P.; Sullivan, L. M.; McAteer, J. B.; Fox, C. S.; Dupuis, J.; Manning, A. K.; Florez, J. C.; Wilson, P. W.; D'Agostino, R. S.; Cupples, L. A. Genotype score in addition to common risk factors for prediction of type 2 diabetes. *N. Engl. J. Med.* **2008**, *359* (21), 2208–2219.
(10) Li, H.; Wu, Y.; Loos, R. J.; Hu, F. B.; Liu, Y.; Wang, J.; Yu, Z.; Lin, X. Variants in the fat mass- and obesity-associated (FTO) gene are not associated with obesity in a Chinese Han population. *Diabetes* **2008**, *57* (1), 264–268.
(11) Nicholson, J. K.; Lindon, J. C.; Holmes, E. 'Metabonomics': understanding the metabolic responses of living systems to pathophysiological stimuli via multivariate statistical analysis of biological NMR spectroscopic data. *Xenobiotica* **1999**, *29* (11), 1181–1189.
(12) Tang, H. R.; Wang, Y. L. Metabonomics-a revolution in progress. *Prog. Biochem. Biophys.* **2006**, *33* (5), 401–417.
(13) Wang, Y.; Holmes, E.; Tang, H.; Lindon, J. C.; Sprenger, N.; Turini, M. E.; Bergonzelli, G.; Fay, L. B.; Kochhar, S.; Nicholson, J. K. Experimental metabonomic model of dietary variation and stress interactions. *J. Proteome Res.* **2006**, *5* (7), 1535–1542.
(14) Qu, Y.; Adam, B. L.; Yasui, Y.; Ward, M. D.; Cazares, L. H.; Schellhammer, P. F.; Feng, Z.; Semmes, O. J.; Jr Wright, G. L. Boosted decision tree analysis of surface-enhanced laser desorption/ionization mass spectral serum profiles discriminates prostate cancer from noncancer patients. *Clin. Chem.* **2002**, *48* (10), 1835–1843.
(15) Yap, I. K.; Clayton, T. A.; Tang, H.; Everett, J. R.; Hanton, G.; Provost, J. P.; Le, N. J.; Charuel, C.; Lindon, J. C.; Nicholson, J. K. An integrated metabonomic approach to describe temporal metabolic disregulation induced in the rat by the model hepatotoxin allyl formate. *J. Proteome Res.* **2006**, *5* (10), 2675–2684.
(16) Bundy, J. G.; Lenz, E. M.; Bailey, N. J.; Gavaghan, C. L.; Svendsen, C.; Spurgeon, D.; Hankard, P. K.; Osborn, D.; Weeks, J. M.; Trauger, S. A.; Speir, P.; Sanders, I.; Lindon, J. C.; Nicholson, J. K.; Tang, H. Metabonomic assessment of toxicity of 4-fluoroaniline, 3,5-difluoroaniline and 2-fluoro-4-methylaniline to the earthworm Eisenia veneta (Rosa): identification of new endogenous biomarkers. *Environ. Toxicol. Chem.* **2002**, *21* (9), 1966–1972.
(17) Yang, Y.; Li, C.; Nie, X.; Feng, X.; Chen, W.; Yue, Y.; Tang, H.; Deng, F. Metabonomic studies of human hepatocellular carcinoma using high-resolution magic-angle spinning ^{1}H NMR spectroscopy in conjunction with multivariate data analysis. *J. Proteome Res.* **2007**, *6* (7), 2605–2614.
(18) Chen, W. X.; Lou, H. Y.; Zhang, H. P.; Nie, X.; Xiang, Y.; Yang, Y. X.; Wu, G. Y.; Qi, J. P.; Yue, Y.; Lei, H.; Tang, H. R.; Deng, F. Metabonomic characterization of the low-grade human astrocytomas and meningiomas using magic-angle spinning ^{1}H nuclear magnetic resonance spectroscopy and principal component analysis. *Prog. Biochem. Biophys.* **2006**, *35* (10), 1142–1153.
(19) Brindle, J. T.; Antti, H.; Holmes, E.; Tranter, G.; Nicholson, J. K.; Bethell, H. W.; Clarke, S.; Schofield, P. M.; McKilligin, E.; Mosedale, D. E.; Grainger, D. J. Rapid and noninvasive diagnosis of the presence and severity of coronary heart disease using ^{1}H-NMR-based metabonomics. *Nat. Med.* **2002**, *8* (12), 1439–1444.
(20) Wang, Y.; Holmes, E.; Nicholson, J. K.; Cloarec, O.; Chollet, J.; Tanner, M.; Singer, B. H.; Utzinger, J. Metabonomic investigations

in mice infected with *Schistosoma mansoni*: an approach for biomarker identification. *Proc. Natl. Acad. Sci. U.S.A.* **2004**, *101* (34), 12676–12681.
(21) Wang, Y.; Utzinger, J.; Saric, J.; Li, J. V.; Burckhardt, J.; Dirnhofer, S.; Nicholson, J. K.; Singer, B. H.; Brun, R.; Holmes, E. Global metabolic responses of mice to *Trypanosoma brucei brucei* infection. *Proc. Natl. Acad. Sci. U.S.A.* **2008**, *105* (16), 6127–6132.
(22) Li, J. V.; Holmes, E.; Saric, J.; Keiser, J.; Dirnhofer, S.; Utzinger, J.; Wang, Y. Metabolic profiling of a *Schistosoma mansoni* infection in mouse tissues using magic angle spinning-nuclear magnetic resonance spectroscopy. *Int. J. Parasitol.* **2009**, *39* (5), 547–558.
(23) Nicholson, J. K.; O'Flynn, M. P.; Sadler, P. J.; Macleod, A. F.; Juul, S. M.; Sonksen, P. H. Proton-nuclear-magnetic-resonance studies of serum, plasma and urine from fasting normal and diabetic subjects. *Biochem. J.* **1984**, *217* (2), 365–375.
(24) Wang, C.; Kong, H.; Guan, Y.; Yang, J.; Gu, J.; Yang, S.; Xu, G. Plasma phospholipid metabolic profiling and biomarkers of type 2 diabetes mellitus based on high-performance liquid chromatography/electrospray mass spectrometry and multivariate statistical analysis. *Anal. Chem.* **2005**, *77* (13), 4108–4116.
(25) Yang, J.; Xu, G.; Hong, Q.; Liebich, H. M.; Lutz, K.; Schmulling, R. M.; Wahl, H. G. Discrimination of Type 2 diabetic patients from healthy controls by using metabonomics method based on their serum fatty acid profiles. *J. Chromatogr., B.: Anal. Technol. Biomed. Life Sci.* **2004**, *813* (1−2), 53–58.
(26) Qiu, Y.; Rajagopalan, D.; Connor, S, C.; Damian, D.; Zhu, L.; Handzel, A.; Hu, G.; Amanullah, A.; Bao, S.; Woody, N.; MacLean, D.; Lee, K.; Vanderwall, D.; Ryan, T. Multivariate classification analysis of metabolomic data for candidate biomarker discovery in type 2 diabetes mellitus. *Metabolomics* **2008**, *4*, 337–346.
(27) Dumas, M.; Barton, R. H.; Toye, A.; Cloarec, O.; Blancher, C.; Rothwell, A.; Fearnside, J.; Tatoud, R.; Blanc, V.; Lindon, J. C.; Mitchell, S.; Holmes, E.; McCarthy, M.; Scott, J.; Gauguier, D.; Nicholson, J. K. Metabolic profiling reveals a contribution of gut microbiota to fatty liver phenotype in insulin-resistant mice. *Proc. Natl. Acad. Sci. U.S.A.* **2006**, *103* (33), 12511–12516.
(28) Li, M.; Wang, B.; Zhang, M.; Rantalainen, M.; Wang, S.; Zhou, H.; Zhang, Y.; Shen, J.; Pang, X.; Zhang, M.; Wei, H.; Chen, Y.; Lu, H.; Zuo, J.; Su, M.; Qiu, Y.; Jia, W.; Xiao, C.; Smith, L. M.; Yang, S.; Holmes, E.; Tang, H.; Zhao, G.; Nicholson, J. K.; Li, L.; Zhao, L. Symbiotic gut microbes modulate human metabolic phenotypes. *Proc. Natl. Acad. Sci. U.S.A.* **2008**, *105* (6), 2117–2122.
(29) Martin, F. P.; Dumas, M. E.; Wang, Y.; Legido-Quigley, C.; Yap, I. K.; Tang, H.; Zirah, S.; Murphy, G. M.; Cloarec, O.; Lindon, J. C.; Sprenger, N.; Fay, L. B.; Kochhar, S.; van Bladeren, P.; Holmes, E.; Nicholson, J. K. A top-down systems biology view of microbiome-mammalian metabolic interactions in a mouse model. *Mol. Syst. Biol.* **2007**, *3*, 112.
(30) Makinen, V. P.; Soininen, P.; Forsblom, C.; Parkkonen, M.; Ingman, P.; Kaski, K.; Groop, P. H.; Ala-Korpela, M. ^{1}H NMR metabonomics approach to the disease continuum of diabetic complications and premature death. *Mol. Syst. Biol.* **2008**, *4*, 167.
(31) Shaham, O.; Wei, R.; Wang, T. J.; Ricciardi, C.; Lewis, G. D.; Vasan, R. S.; Carr, S. A.; Thadhani, R.; Gerszten, R. E.; Mootha, V. K. Metabolic profiling of the human response to a glucose challenge reveals distinct axes of insulin sensitivity. *Mol. Syst. Biol.* **2008**, *4*, 214.
(32) Alberti, K. G.; Zimmet, P. Z. Definition, diagnosis and classification of diabetes mellitus and its complications. Part 1: diagnosis and classification of diabetes mellitus provisional report of a WHO consultation. *Diabet. Med.* **1998**, *15* (7), 539–553.
(33) Matthews, D. R.; Hosker, J. P.; Rudenski, A. S.; Naylor, B. A.; Treacher, D. F.; Turner, R. C. Homeostasis model assessment: insulin resistance and beta-cell function from fasting plasma glucose and insulin concentrations in man. *Diabetologia* **1985**, *28* (7), 412–419.
(34) Meiboom, S.; Gill, D. Modified spin-echo method for measuring nuclear relaxation times. *Rev. Sci. Instrum.* **1958**, *29* (8), 688–691.
(35) Trygg, J.; Wold, S. Orthogonal projections to latent structures (O-PLS). *J. Chemom.* **2002**, *16* (3), 119–128.
(36) Cloarec, O.; Dumas, M. E.; Trygg, J.; Craig, A.; Barton, R. H.; Lindon, J. C.; Nicholson, J. K.; Holmes, E. Evaluation of the orthogonal projection on latent structure model limitations caused by chemical shift variability and improved visualization of biomarker changes in ^{1}H NMR spectroscopic metabonomic studies. *Anal. Chem.* **2005**, *77* (2), 517–526.
(37) Eriksson, L.; Johansson, E.; Kettaneh-Wold, N.; Trygg, J.; Wikstrom, C.; Wold, S.; *Multi- and Megavariate Data Analysis. Part I. Basic Principles and Applications*, 2nd ed.; Umetrics Academy: Umea, Sweden, 2006.
(38) Tang, H.; Wang, Y.; Nicholson, J. K.; Lindon, J. C. Use of relaxation-edited one-dimensional and two dimensional nuclear magnetic resonance spectroscopy to improve detection of small metabolites in blood plasma. *Anal. Biochem.* **2004**, *325* (2), 260–272.
(39) Nicholson, J. K.; Foxall, P. J.; Spraul, M.; Farrant, R. D.; Lindon, J. C. 750 MHz ^{1}H and ^{1}H-^{13}C NMR spectroscopy of human blood plasma. *Anal. Chem.* **1995**, *67* (5), 793–811.
(40) Cline, G. W.; Petersen, K. F.; Krssak, M.; Shen, J.; Hundal, R. S.; Trajanoski, Z.; Inzucchi, S.; Dresner, A.; Rothman, D. L.; Shulman, G. I. Impaired glucose transport as a cause of decreased insulin-stimulated muscle glycogen synthesis in type 2 diabetes. *N. Engl. J. Med.* **1999**, *341* (4), 240–246.
(41) Cusi, K.; Consoli, A.; DeFronzo, R. A. Metabolic effects of metformin on glucose and lactate metabolism in noninsulin-dependent diabetes mellitus. *J. Clin. Endocrinol. Metab.* **1996**, *81* (11), 4059–4067.
(42) Perseghin, G.; Ghosh, S.; Gerow, K.; Shulman, G. I. Metabolic defects in lean nondiabetic offspring of NIDDM parents: a cross-sectional study. *Diabetes* **1997**, *46* (6), 1001–1009.
(43) Gougeon, R.; Morais, J. A.; Chevalier, S.; Pereira, S.; Lamarche, M.; Marliss, E. B. Determinants of whole-body protein metabolism in subjects with and without type 2 diabetes. *Diabetes Care* **2008**, *31* (1), 128–133.
(44) Krebs, M.; Brehm, A.; Krssak, M.; Anderwald, C.; Bernroider, E.; Nowotny, P.; Roth, E.; Chandramouli, V.; Landau, B. R.; Waldhausl, W.; Roden, M. Direct and indirect effects of amino acids on hepatic glucose metabolism in humans. *Diabetologia* **2003**, *46* (7), 917–925.
(45) Garvey, W. T.; Kwon, S.; Zheng, D.; Shaughnessy, S.; Wallace, P.; Hutto, A.; Pugh, K.; Jenkins, A. J.; Klein, R. L.; Liao, Y. Effects of insulin resistance and type 2 diabetes on lipoprotein subclass particle size and concentration determined by nuclear magnetic resonance. *Diabetes* **2003**, *52* (2), 453–462.
(46) Kotronen, A.; Juurinen, L.; Tiikkainen, M.; Vehkavaara, S.; Yki-Järvinen, H. Increased liver fat, impaired insulin clearance, and hepatic and adipose tissue insulin resistance in type 2 diabetes. *Gastroenterology* **2008**, *135* (1), 122–130.
(47) Leite, N. C.; Salles, G. F.; Araujo, A. L.; Villela-Nogueira, C. A.; Cardoso, C. R. Prevalence and associated factors of non-alcoholic fatty liver disease in patients with type-2 diabetes mellitus. *Liver Int.* **2009**, *29* (1), 113–119.
(48) Buchman, A. L.; Dubin, M. D.; Moukarzel, A. A.; Jenden, D. J.; Roch, M.; Rice, K. M.; Gornbein, J.; Ament, M. E. Choline deficiency: a cause of hepatic steatosis during parenteral nutrition that can be reversed with intravenous choline supplementation. *Hepatology* **1995**, *22* (5), 1399–1403.

PR900524Z